Precision Engineering 88 (2024) 241–250

Contents lists available at ScienceDirect

Precision Engineering

journal homepage: www.elsevier.com/locate/precision

Post-process updating of model parameters to approximate thermal errors of machine tools operating in different configurations

Daniel Divíšek, Martin Mareš *, Otakar Horejš

Czech Technical University in Prague, Faculty of Mechanical Engineering, Department of Production Machines and Equipment, RCMT, Horská 3, 128 00 Prague, Czech Republic

ARTICLE INFO

Handling editor: S Ludwick

Keywords:
Machine tool
Thermal error
Updating
Repetitive production

ABSTRACT

Machine tool (MT) thermal errors induced by external and internal heat sources (e.g. changing environment, friction and power losses in MT components) are an important element in machined workpiece inaccuracies. In the past few decades, indirect software compensation techniques have been used to address thermal errors on account of their economic and ecological aspects. Many slightly different approaches are described in the literature. If thermal error models are properly identified based on experiments with sufficiently varying input parameters, they usually work within similar calibration and verification conditions. As the sensory equipment of machines increases, models can be adapted to regions with higher thermo-mechanical system nonlinearity and inhomogeneity through the introduction of deformation feedback from direct measurements into model structures. However, adaptive functionalities require discrete interruptions of the MT's work cycle, which threaten the integrity of the machined surface and complicate the model structure and thus also implementation and industrial deployment possibilities. In this research, a novel approach of automatic post-process adaptation suitable for repetitive manufacturing, which takes advantage of transfer functions (TF), is proposed for thermal error reduction. The method respects basic heat transfer mechanisms in the MT structure by combining linear parametric models, requires a minimum of additional gauges, and feedback from direct measurements is obtained only during technological pauses in the production process. Post-process adaptation is solved retrospectively by updating model parameters using the heuristic method of genetic algorithms (GA). First, the approach was tuned on a case study of a heavy-duty milling machine with a horizontal headstock for a configuration with an exchangeable spindle head and a configuration with a change in the position of the headstock in the workspace, both of which were different from the initial model's calibration range. Subsequently, the developed approach was applied to repeated production on a medium-sized milling centre. Another goal of the paper is to emphasize the need for quality input information for modelling efforts and the industrial applicability of scientific results.

1. Introduction

A machine tool (MT) can be considered a rigid system. However, various dynamic phenomena resulting in structural deformations load the machine during working processes. In addition to errors caused by manufacturing and assembly inaccuracies, the machine is exposed to three categories of deformations [1].

- Static errors related to the static rigidity of the machine and its structure including errors that form between the tool and the workpiece, e.g. from component wear, workpiece displacement, etc.
- Dynamic errors arising with the machining process. The magnitude of these errors depends on the dynamic stiffness of the machine, drive adjustment and setting of cutting conditions.
- Thermal errors induced by conduction, convection and radiation heat transfer mechanisms in the MT structure due to the action of external and internal heat sources.

Geometrical and dimensional errors resulting from the activity of non-stationary heat phenomena can be described as deviations from the planned path of the tool and the workpiece. Thermal errors accompanying machine operation account for 40–70% of the total MT inaccuracy detected on the workpiece [2]. Given the significant role that thermal

* Corresponding author.
E-mail address: m.mares@rcmt.cvut.cz (M. Mareš).

https://doi.org/10.1016/j.precisioneng.2024.02.011
Received 20 January 2023; Received in revised form 31 January 2024; Accepted 12 February 2024
Available online 17 February 2024

errors play, one of MT designers' main goals is to minimise these errors.

Generally, solutions to this issue fall into one of the following main groups [3].

- Machine structure optimisation leading to lower sensitivity to heat flow, e.g. Ref. [4].
- Temperature gradient control of the MT and its environment, e.g. Refs. [5,6].
- Compensation of thermal errors, e.g. Ref. [7].

Design modifications include topological optimisation of the machine structure, choice of a suitable material or placement of individual elements such as electric motors, switchboards, power transformers, aggregates, etc. to achieve thermal symmetry. This approach can only be implemented in the prototype stage of a machine. The design and subsequent control of the cooling system play an important role. Using internally cooled frames or individual components such as a spindle or ball screw are common current alternatives to significantly increase product accuracy. However, greater financial and environmental demands are associated with innovating machines with new components and subsequently operating innovated machines. Unlike the previously described approaches, compensations are an economically and ecologically promising way of minimising thermal errors. Two methods of compensating thermal errors at the tool centre point (TCP) can be classified as follows [8].

- Direct compensation.
- Indirect software compensation.

Direct compensations are based on in-process measurement of deformations, e.g. using a touch probe, during production and the subsequent correction of machine axes' programmed positions in real time. Gao et al. presented state-of-the-art on-machine and in-process measurement systems and sensor technologies [9]. The disadvantage is the need to interrupt the process, which prolongs production time and has a negative impact on the integrity of the machined surface.

In contrast, numerous mathematical approaches can be applied in indirect software compensation. The latest research on approaches to thermal error modelling can be found in Mayr [10] and an update covering the last decade is available in Li [11]. A review focused on compensation of spindle thermal errors, which are ordinarily a dominant heat source influencing MT accuracy, can be found in Li [12]. Indirect compensation thermal error models can be based either on numerical simulation results or empirical modelling.

In the case of numerical simulations, partial differential equation (PDE) [13], finite difference method (FDM), finite element method (FEM) or a combination (FDEM) can be applied to investigate the thermal deformation at the TCP [14]. Although they are promising, numerical simulations can be a time-consuming process. An auspicious contemporary approach is to couple FEM with model order reduction (MOR) techniques to reduce the computing time [15]. Cyber physical systems (CPS) of thermal digital twins are the latest vision in the use of numerical methods [16]. Nevertheless, the creation of a complex and nonstationary predictive numerical model of MT thermal errors is still a complicated process, due to many factors, e.g., heat transfer through the joint, establishing the boundary conditions for ambient influence, etc. Therefore, most indirect software compensation strategies are based on empirical models using measured auxiliary variables.

Many strategies have been investigated to establish indirect models in the form of white, black, or grey boxes [17], e.g. multiple regression analysis (MRA) [18], whose simplicity renders it one of the most widely used methods by MT control system producers, transfer functions (TF) [19], phenomenological models employed in the current research, artificial neural networks (ANN) [20], algorithms applied in machine learning principles, etc. The majority of the compensation models introduced in the literature have the potential to significantly reduce MT thermal errors. The methods differ in the amount and type of input variables and time required for model training and architecture. However, the robustness of indirect models can be affected over time by e.g. wear, replacement of components, changes in technological conditions or the operating environment. These inaccuracies can be compensated by implementing deformation feedback from the thermo-mechanical system through direct measurements [21].

With the expansion of machine sensory equipment in the context of Industry 4.0, the combination of both approaches becomes a logical way of increasing the long-term reliability and robustness of compensation models toward intelligent manufacturing. Mayr et al. [22] proposed TF-based thermal error compensation of a 5-axis MT that is extended by on-machine measurements. The information gained by periodic process intermittent probing with a sampling time of 5 min is used to adaptively update the model parameters in real time. Zimmermann et al. [23] replaced the periodicity with a trigger based on temperature measurements when unknown thermal conditions occur. An adaptive input selection method, also developed in Ref. [23], enables automated and adaptive selection of the optimal model inputs even after the initial model training. The TF-based model has a black-box structure that changes with each run of the recalibration cycle independently of the previous model architecture. However short, recalibration still relies on the history of frequent positionally-independent on-machine probing.

At the interface of indirect compensations and models with online adaptive functionalities, there is post-process parameter updating, which depends directly on the specific production process. Post-process updating is commonly used to correct geometric inaccuracies in the toolpath when machining long workpieces. Neumann et al. [24] used load case dependent updates to improve the FEM model structure of a 5-axis machining centre through the creation of an additional unique MRA model for measured residual deformations. The training data for the update were obtained from a dry run of the NC file and periodic measurements of artefacts,e.g. a datum ball in the workspace.

The research presented in this article uses TF-based granular model structures adopted from Ref. [25] to create an indirect compensation model approximating thermal errors caused by spindle rotation of a heavy-duty milling machine with a horizontal headstock. The model is applied to verification testing throughout the spindle speed range in the calibration configuration and in a configuration with the spindle head and a change of spatial position in the machine workspace. Insufficient correlation of the temperature excitation with the deformation response and differences from the calibration measurement are reflected in the reduced model efficiency. The effectiveness of the initial model for repetitive production is increased by post-process adaptation of the model parameters to new situations using gain scheduling [26]. Post-process adaptation is automated using the heuristic method of genetic algorithms (GA), minimising residual deformations in time instants of measurements during technological parameter changes. This reduces intermittent probing that disrupts the continuity of the first production cycle with an active initial model. Updates are easily embedded into the model's preserved structure without increasing modelling requirements.

The introductory section of the paper is followed by an explanation of the target machine suitable for transparent demonstration of the development of the method and experimental set-up for thermo-mechanical measurements. Section 3 deals with the mathematical approach and modelling procedures adopted from Ref. [25], including a thermo-mechanical system analysis and initial TF-based model application to areas outside the calibration range. The development of the post-process update method is elucidated in section 4 along with the improvement that was achieved. In section 5, the advantages of a post-process updated model are illustrated on a case study of repeated production performed on a different MT. A brief summary and future scope of work related to this approach are presented in the final section 6.

2. Experimental set-up and conditions

Two target machines are the subject of this research. The first is a heavy-duty milling machine with a horizontal spindle. The machine's workspace dimensions are 3000x2000 × 2500 mm, it has a maximum spindle speed of 6000 rpm and a maximum of 4000 rpm with an exchangeable spindle head increasing headstock assembly rigidity during drilling operations. The machine bodies are made of cast iron. The schematic machine kinematics and experimental set-up are depicted in Fig. 1.

The first case study focuses on a transparent demonstration of the post-process updated model's capabilities. In this case the model updates were only identified, and three experiments were performed on the first target machine for that purpose.

1) Calibration of the indirect compensation model according to the conditions specified by the international standard ISO 230–3:2020 [27]. The calibration took place in the basic configuration of the spindle loaded with a constant speed of 4000 rpm and consisted of the transient behaviour between two thermodynamic equilibria: first the MT in approximate balance with its surroundings and second the MT steady state during heat source activity, followed by a cooling phase. Both phases were considered in the modelling effort. The machine was set in the first testing position [X0, Y0, Z0, W0]. The impact of ambient temperature changes was also considered in the indirect model structure.
2) Verification experiment of the MT in the basic configuration set in the first testing position [X0, Y0, Z0, W0]. The experimental set-up consisted of variable spindle speed spectra with a speed change every 1 h through the whole range up to 6000 rpm. The aim of the test was to verify the linearity between the inputs and outputs of the thermo-mechanical system within the calibration conditions.
3) Verification experiment of the MT set in the second testing position [X0, Y+1049, Z0, W0] and equipped with an exchangeable spindle head. The experimental set-up consisted also of variable spindle speed spectra with speed changes every 1 h through the whole range up to 4000 rpm. The aim of the test was to observe the change in the thermo-mechanical system homogeneity due to the differences in the axial configurations and machine modularity compared to the previous tests.

An angle for mounting the measuring device in the two testing positions was placed on the table. The measuring device consists of a measuring fixture containing 5 PR6423 Eddy-current sensors used for

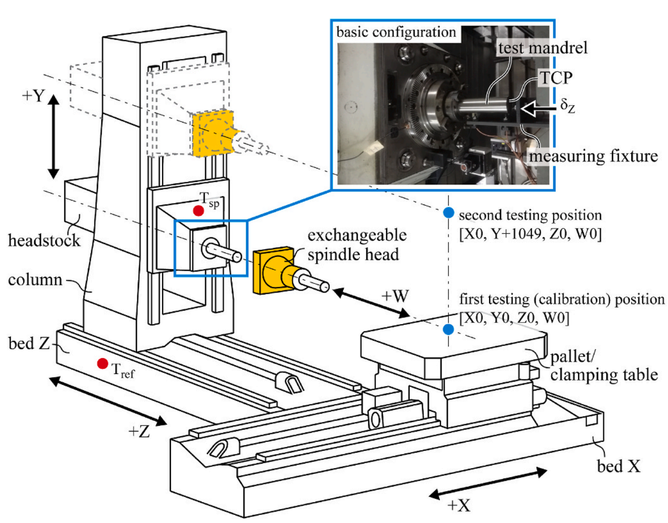

Fig. 1. Schema of a heavy-duty milling machine with a horizontal headstock in various axis configurations for spatial thermal error measurements.

noncontact sensing of displacements in the X, Y and Z directions between the angle and the TCP of the test mandrel clamped in the spindle, as shown in Fig. 1. The angle represents the clamped workpiece and emphasises the need to obtain the correct measured values of system feedback for effective adaptation of the thermal error model.

The second case study concerns a medium-sized 5-axis milling centre similar to the target machine in Ref. [28] with workspace dimensions of 700x820 × 550 mm, 24000 rpm maximum spindle speed and CAFYXZ machine axial arrangement. The goal here was to apply the developed post-process adaptation strategy to a drill-like test with a repeated NC program while considering, in comparison to the calibration set-up, start-stop spindle activity at maximum speed and the presence of a process liquid.

All experiments were performed under idle load conditions, i.e. no cutting process involved. The results focused on thermal errors in the most affected machine axis, Z (W), corresponding to the tool axis elongation. Deformations were expressed in relative values due to data confidentiality.

3. Indirect compensation model structure

3.1. Mathematical approach

The concept behind the modelling approach is based on usage of a minimum of additional gauges which means only signals from the MT control system [19], an open structure that is easy to extend, modify and advantageous for machine-learning principles [29], real time application and ease of implementation into MT control systems.

A compensation strategy based on the theory of TFs, widely used in electrical and mechanical systems [30], is a dynamic method capable of approximating the analytical solution to the fundamental generalised problem (FGP) of the heat transfer in the MT structure with sufficient accuracy [31]. A discrete TF is used to describe the link between the excitation, here a temperature difference, and its response, a deformation in this case:

$$y(t) = \varepsilon \bullet u(t) + e(t). \tag{1}$$

The vector u(t) in equation (1) is the TF input and y(t) is the output vector in the time domain, ε represents the general TF in the time domain, and e(t) is the disturbance value, which is further neglected. The TF form of the polynomials' quotient is expressed by equation (2).

$$\frac{Z\{y(t)\}}{Z\{u(t)\}} = \frac{a_n \bullet z^{-n} + \cdots + a_1 \bullet z^{-1} + a_0 \bullet z^0}{b_m \bullet z^{-m} + \cdots + b_2 \bullet z^{-2} + b_1 \bullet z^{-1} + b_0 \bullet z^0}, \tag{2}$$

where Z is the Z-transform of the time discretised function, z is the complex variable, n is the order of the TF numerator, m is the order of the TF denominator, and it holds that $m > n$. Further, $a_{0:n}$ are the calibration coefficient of the TF input, and $b_{0:m}$ are the calibration coefficient of the TF output. The difference form of the discrete TF in the time domain is introduced in equation (3). This form is generally suitable for modern MT control systems using their programming languages.

$$y(k) = \frac{u(k-n) \bullet a_n + \cdots + u(k-1) \bullet a_1 + u(k) \bullet a_0}{b_0} - \left(\frac{y(k-m) \bullet b_m + \cdots + y(k-1) \bullet b_1}{b_0}\right), \tag{3}$$

where k represents the examined time instant and k-n (k-m) is the n-multiple (m-multiple) delay in the sampling frequency of the measured input vector (simulated output vector). The sampling frequency is equal to 1 s^{-1} in the article. A linear parametric model with an autoregressive with extra input (ARX) identifying structure is used with the help of *Matlab Identification Toolbox* [32]. The ARX as an optimal model structure with the best fit in quality and robustness is also discussed in Ref. [22].

The approximation quality of the simulated behaviour is expressed by a global approach based on a normalised root mean squared error (NRMSE) method *fit* [32] as expressed in equation (4). The *fit* is a percentage value of model efficiency where 100% would equal a perfect match of the measured and simulated behaviours:

$$fit = \left(1 - \frac{\|y_{mea} - y_{sim}\|}{\|y_{mea} - \overline{y}_{mea}\|}\right) \bullet 100. \tag{4}$$

The y_{mea} value in equation (4) is the measured output - displacements in the machine direction Z in this case, y_{sim} is the simulated model output, and $\overline{y}_{mea}$ expresses the arithmetic mean of the measured output over time.

3.2. Initial indirect compensation model for thermal errors

An indirect compensation model approximating thermal errors induced by spindle rotation without an exchangeable spindle head distinguishes, in addition to a separate compensation component for the ambient temperature influence, between the heating and cooling phases in a form derived from Ref. [25]. The differences between phases are due to the presence of the forced convection in the heating phase caused by the rotating parts of the MT. The indirect model structure is given in equation (5).

$$\Sigma\delta_{Z\ sim} = \underbrace{\Delta T_{ref} \bullet \varepsilon_{Z\ amb}}_{\delta_{Z\ sim\ amb}} + \underbrace{\underbrace{\left(\Delta T_{sp} - \Delta T_{ref}\right) \bullet \varepsilon_{Z\ cool}}_{\delta_{Z\ sim\ cool}} + \underbrace{g_n \bullet \left(\Delta T_{sp} - \Delta T_{ref}\right) \bullet \varepsilon_{Z\Delta}}_{\Delta\delta_{Z\ sim}}}_{\delta_{Z\ sim\ sp}}, \text{ where}$$
$$g_n = 1 \Leftrightarrow n > 0 \vee g_n = 0 \Leftrightarrow n = 0. \tag{5}$$

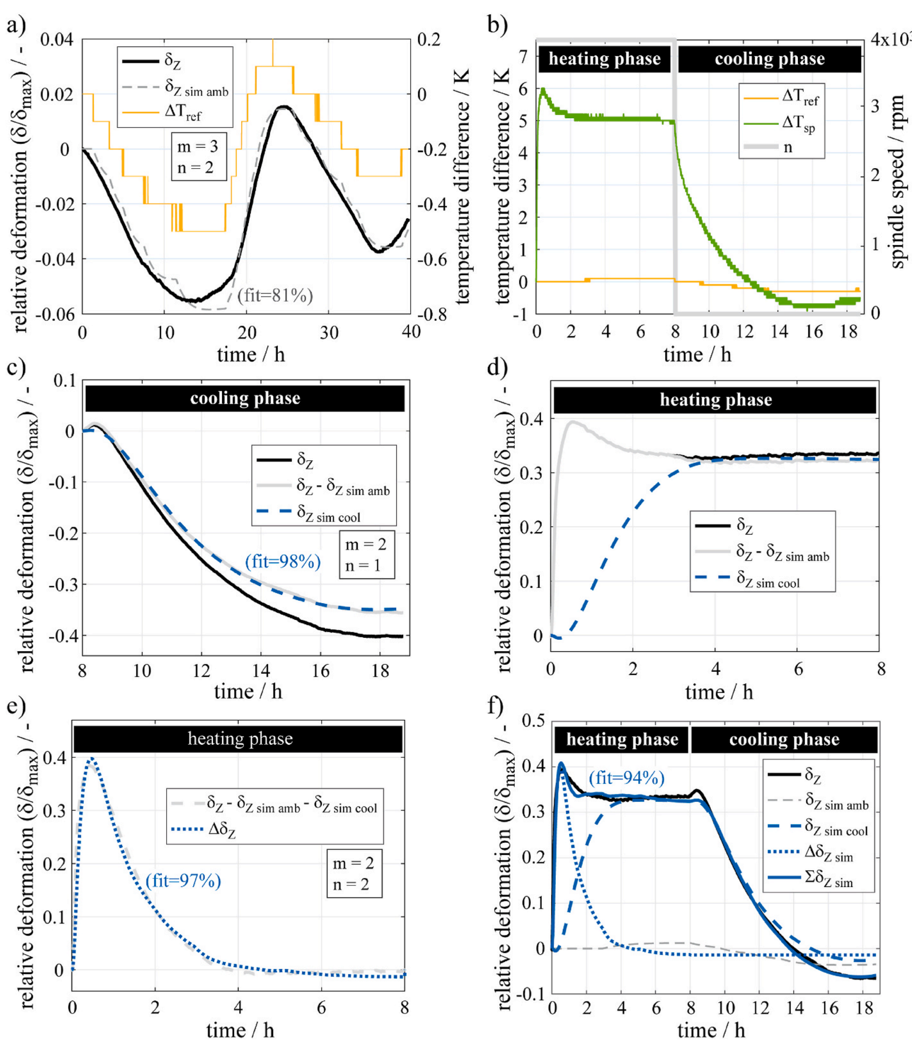

Fig. 2. Procedure of developing an indirect compensation model of the machine's thermo-mechanical behaviour in the Z-axis caused by spindle rotation: a) identification of the deformation component from the surrounding environment, b) input quantities during the calibration measurement, c) identification of the deformation component of the cooling phase, d) difference between the heating and cooling phases, e) identification of the deformation component of the phase difference, f) resulting description.

The quantities ΔT_{ref} reflecting changes in ambient and ΔT_{sp} measured close to the spindle front bearings are inputs to equation (5) model in the form of temperature changes. The approximate positions of the temperature probes on the target machine are shown in Fig. 1; both are embedded in the control system by the MT builder. Designations $\varepsilon_{Z\ amb}$, $\varepsilon_{Z\ cool}$ and $\varepsilon_{Z\Delta}$ correspond to identified discrete TFs in the time domain. The principle of the indirect compensation model calibration is presented in Fig. 2.

First, the deformation component $\delta_{Z\ sim\ amb}$ in equation (5) caused by the change in ambient temperature during the ETVE test [27] was identified (Fig. 2 a)). This component was further subtracted from the measured deformations $\delta_{Z\ TCP}$ during the calibration of the spindle rotation influence. The calibration measurement was taken in the first testing position [X0, Y0, Z0, W0] at a constant spindle speed of 4000 rpm, followed by the cooling phase (Fig. 2 b)). The TF $\varepsilon_{Z\ cool}$ of the separate cooling phase was identified from part of the calibration measurement (Fig. 2 c)). The cooling phase sub-model $\delta_{Z\ sim\ cool}$ was then applied to the heating phase behaviour (Fig. 2 d)). The difference between the measured and simulated deformations in the heating phase $\Delta\delta_Z$ is the response of the second identified TF $\varepsilon_{Z\Delta}$ to approximate the effect of the spindle rotation $\delta_{Z\ sim\ sp}$ (Fig. 2 e)). The resulting description $\Sigma\delta_{Z\ sim}$ from equation (5) is the sum of all three components (Fig. 2 f)). The component $\Delta\delta_{Z\ sim}$ is inactive during the cooling phase. Therefore, the coefficient g_n is present in equation (5) as a function of the spindle speed n. The graphs in Fig. 2 contain the orders of the identified TFs and the global approximation quality indicator *fit* achieved during the identification process.

The indirect model input and spindle speed behaviour during the verification experiment of the MT in the basic configuration set in the first testing position [X0, Y0, Z0, W0] and the measured, simulated and residual deformations are depicted in Fig. 3. The area of the residual error is given by the difference between the measured deformation at the TCP in the MT uncompensated state and the output simulated by the model. The residue is expressed as an absolute value for greater comparison possibilities.

Fig. 3 shows that the indirect model's efficiency is $fit = 35\%$. The inaccuracy of the model even in conditions similar to the calibration is caused by insufficient correlation between the temperature input of the indirect model and the measured deformation at the TCP.

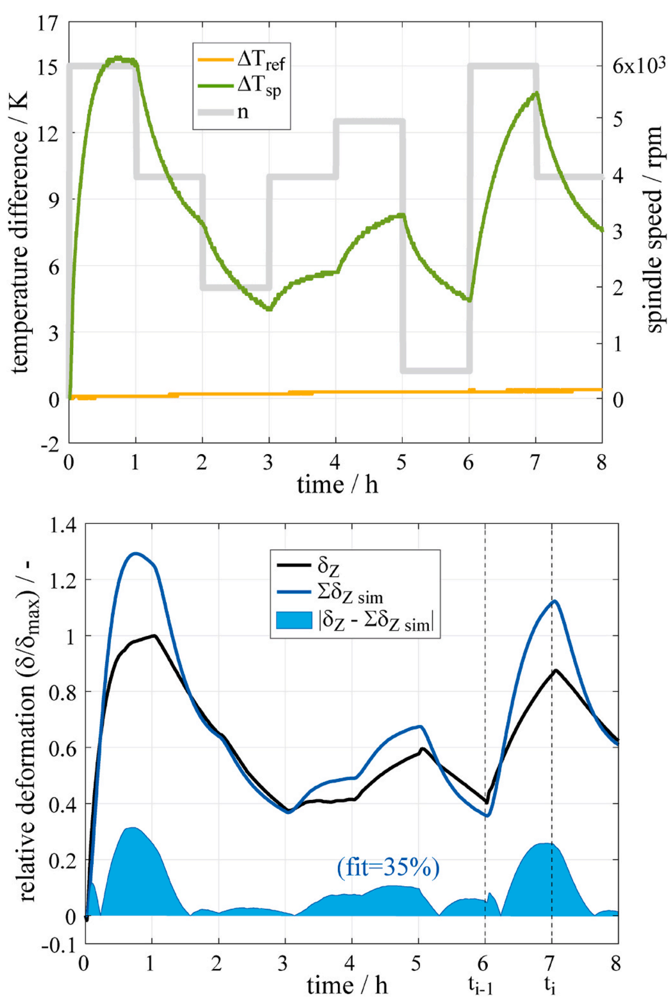

Fig. 3. Input quantities of the indirect compensation model (left) and measured, simulated and residual deformations (right) during the verification test of the machine in the basic configuration.

4. Post-process update of model parameters

Equation (5) can be modified into a post-process adaptive form by applying a pair of gain coefficients g_1 and g_2 as expressed in equation (6). The advantage of the model structure from equation (6) is the possibility of modifying the magnitude of the approximation value and also of adapting the time constant of the simulation to the approximated phenomenon (within the limits of the difference between the heating and cooling phases).

$$\Sigma\delta_{Z\ sim}(g_{1,2}) = \Delta T_{ref} \bullet \varepsilon_{Z\ amb} + \left[\left(\Delta T_{sp} - \Delta T_{ref}\right) \bullet \varepsilon_{Z\ cool}\right] \bullet g_1 + \left[g_n \bullet \left(\Delta T_{sp} - \Delta T_{ref}\right) \bullet \varepsilon_{Z\Delta}\right] \bullet g_2, \tag{6}$$

where the gain coefficients g_1 of cooling phase sub-model $\delta_{Z\ sim\ cool}$ and g_2 of sub-model $\Delta\delta_{Z\ sim}$ of heating and cooling phase difference are, for this

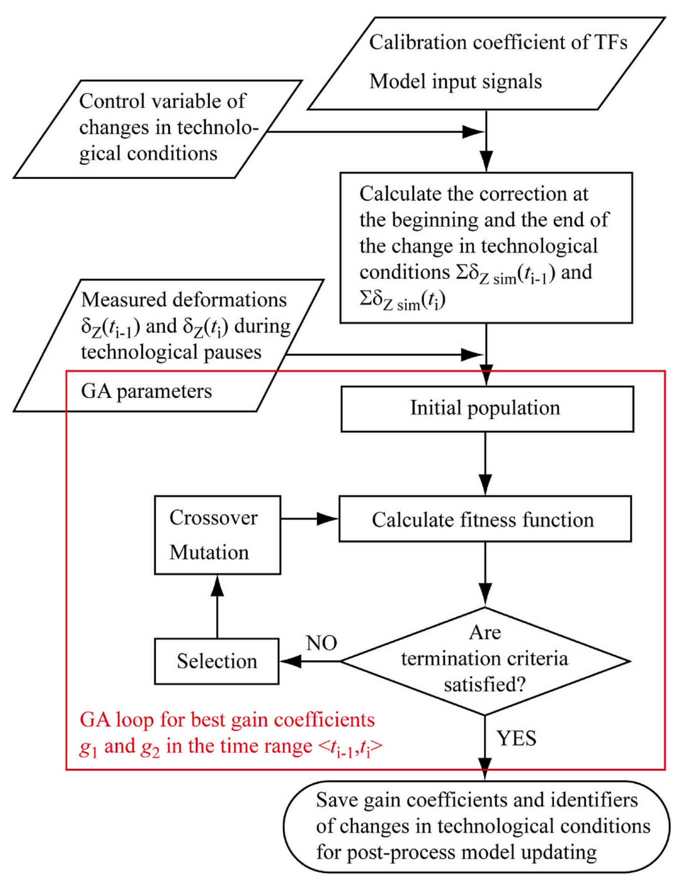

Fig. 4. Flow chart of GA optimisation for automatic post-process parameter updating of the indirect compensation model.

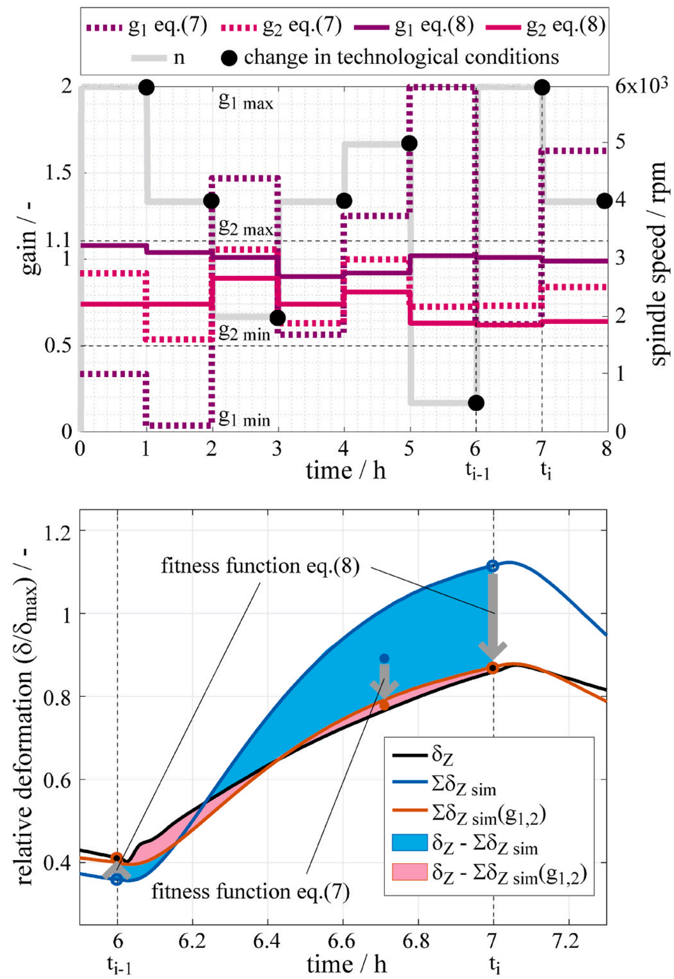

Fig. 5. Procedure of post-process adaptation to the verification test of the machine in the basic configuration: course of the optimised gain coefficients with marking of in-process measurement moments, mean, upper and lower optimisation boundaries (left) and detail of measured and simulated deformations before and after post-process adaptation (right).

case study, functions of the spindle position in the machine's Y axis, the time duration of one operation under certain technological conditions, spindle speed including the history of previous changes and the current equipment of the machine. A Flow chart of post-process adaptation is depicted in Fig. 4.

The pair of gain coefficients is not consistent over time even for the same changes in technological parameters occurring in different sections of the adapted production process, due to inhomogeneous heat propagation through the MT structure and component. Genetic algorithms inspired by evolutionary biology [33] are used to optimise g_1 and g_2 gain coefficients. Successive solutions are formed in each generation and the solutions are improved through gradual evolution to meet a termination criteria of a fitness function within specified boundaries. The criteria of the fitness function is to minimise residues between the measured δ_Z and simulated $\Sigma\delta_{Z\,sim}(g_{1,2})$ values as shown in right part of Fig. 5 on the interval t_{i-1} to t_i defined in Fig. 3. To find characteristic boundaries of the gain coefficients, the test of the machine in the basic configuration is subjected to optimisation using a fitness function from equation (7) maximizing the *fit* value in all time intervals t_{i-1} to t_i between changes in technological conditions represented by spindle speed variations in this case as shown in left part of Fig. 5 by the black dots. The default boundaries of both gain coefficients are set to $g_{1,2} \in \langle 0,2\rangle$. The result of GA optimisation according to fitness function from equation (7) of the gain coefficient values for the test of the machine in the basic configuration is shown in the left part of Fig. 5 with thick dotted lines of purple and pink colours. The resultant characteristic boundaries of the gain coefficients are marked in the figure by the values of $g_{1,2\,min}$ and $g_{1,2\,max}$, namely $g_1 \in \langle 0,2\rangle$ and $g_2 \in \langle 0.5,1.1\rangle$. It is further assumed that optimal solutions lie exactly within these boundaries, otherwise it would be necessary to identify new sub-models with more appropriate inputs for a specific MT configuration.

$$\underset{g_{1,2}\in\langle 0,2\rangle}{\arg\max}\left[\left(1-\frac{\left\|\delta_Z-\Sigma\delta_{Z\,sim}(g_{1,2})\right\|}{\left\|\delta_Z-\bar{\delta}_Z\right\|}\right)\bullet 100\right]_{t_{i-1}}^{t_i}. \tag{7}$$

However, the fitness function from equation (7) considers the continuous acquisition of the measured deformation. This condition limits the use of equation (7) in practical applications. The purpose of GA is to simultaneously minimise the residuals between the measured and simulated values only at the time instants t_{i-1} and t_i according to the fitness function in equation (8) within the previously determined characteristic boundaries, where i indicates the moments of changes in technological conditions. This approach enables post-process adaptation of model parameters with minimal intervention in production.

$$\underset{g_1\in\langle 0,2\rangle,\ g_2\in\langle 0.5,1.1\rangle}{\arg\min}\left[\left|\delta_Z(t_{i-1})-\Sigma\delta_{Z\,sim}(g_{1,2},t_{i-1})\right|+\left|\delta_Z(t_i)-\Sigma\delta_{Z\,sim}(g_{1,2},t_i)\right|\right]. \tag{8}$$

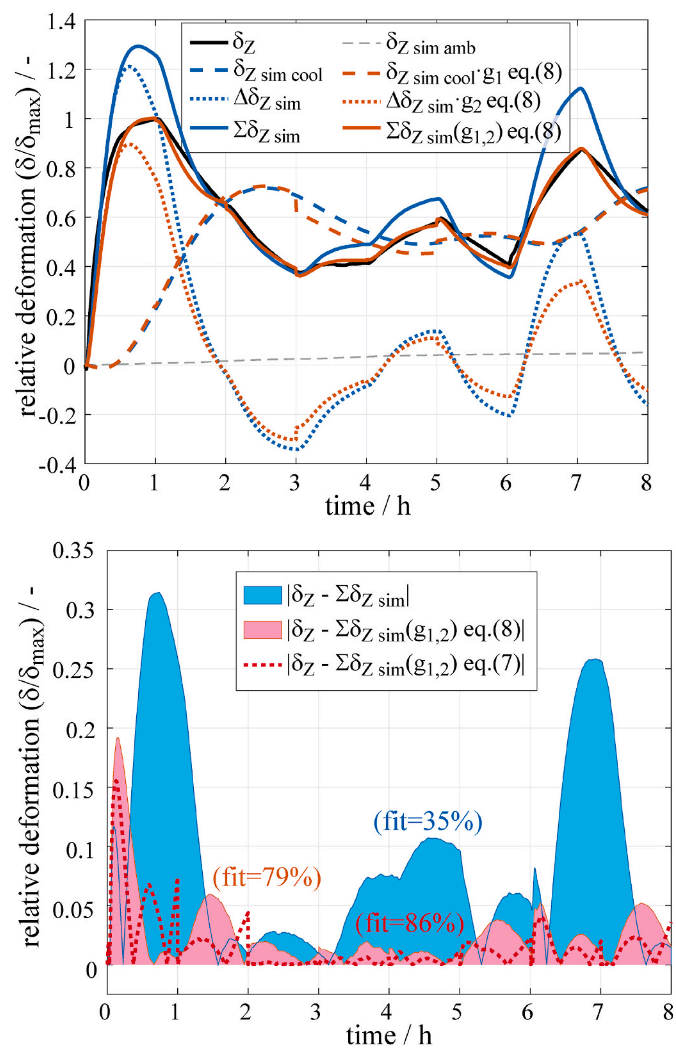

Fig. 6. Measured uncompensated deformations and approximations by the indirect and the post-process updated models with analysis of sub-model behaviours (left) and residuals (right) during the verification test of the machine in the basic configuration.

Optima are found in no more than 30 generations of 500 individuals. The gain coefficients found in the described manner of setting the technological conditions from the verification test introduced in Fig. 3 are shown in left part of Fig. 5 by purple and pink curves. Both courses lie within characteristic boundaries.

The enhanced efficiency of the compensation model from equation (6) with post-process update parameters applied to the same test of Fig. 3 where the gain coefficients g_1 and g_2 were identified is shown in Fig. 6. The left part of Fig. 6 contains analysis of sub-models from equations (5) and (6) resulting in approximations by indirect model with and without post-process updated parameters. The right part of Fig. 6 depicts residuals after applications of models from equation (5) and equation (6) with post-process updated parameters using equation (8) as the fitness function. For comparison, the hypothetical residual resulting from the application of the model optimised by equation (7) fitness function is depicted in red dotted curve.

The model efficiency increases from the initial $fit = 35\%$ to $fit = 79\%$ owing to the post-process update. The efficiency of the optimised model by equation (7) considering continuous deformation behaviour is equal to 86%. From the comparison of the results of both optimisation criteria, it can be concluded that the post-process updated model is sufficiently effective. The achievement of the high efficiency will be evident in repeated production. The issue will be discussed in chapter 5.

The same post-process update procedure is applied to the compensation model for effective approximation of thermal errors induced during another verification test containing significant differences from the model calibration range. The difference consists of machine modularity and the change in the MT axis configuration. The experimental set-up related to this part of the research is depicted in Fig. 7. The MT's headstock equipped with exchangeable spindle head is shown on the left along with the second MT testing position [X0, Y+1049, Z0, W0]. The right part of the figure shows the progress of technological conditions and temperature inputs to the models from equations (5) and (6).

Fitness function from equation (8) with default boundaries of both gain coefficients $g_{1,2} \in \langle 0, 2\rangle$ is given in equation (9). Comparing the result with the optimisation from equation (8) will allow to qualify the benefit of the set characteristic boundaries to gain coefficient $g_2 \in \langle 0.5, 1.1\rangle$.

$$\underset{g_{1,2}\in\langle 0,2\rangle}{\arg\min}\left[\left|\delta_Z(t_{i-1}) - \Sigma\delta_{Z\ sim}(g_{1,2}, t_{i-1})\right| + \left|\delta_Z(t_i) - \Sigma\delta_{Z\ sim}(g_{1,2}, t_i)\right|\right] \tag{9}$$

The results for the experimental set-up under the conditions shown in Fig. 7 are depicted in Fig. 8. The courses of post-process optimised gain coefficients g_1 and g_2 by equations (8) and (9) are presented in the left part of Fig. 8 above the spindle speed with denoted time instants of changes in technological conditions. The measured thermal errors in the Z direction, simulated deformation models from equations (5) and (6) and the residues that would remain after applying the initial model and models optimised according to both boundaries from equations (8) and (9) are shown in the right part of the same figure.

The model efficiency increases from the initial $fit = 41\%$ to $fit = 77\%$

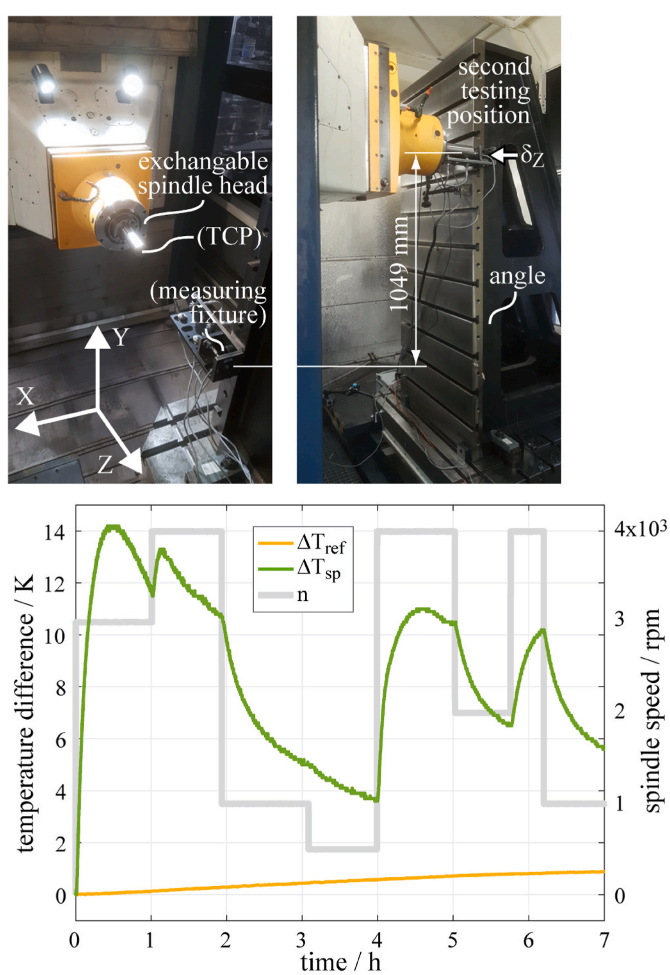

Fig. 7. Input quantities of the compensation models during verification test of the machine equipped with an exchangeable spindle head in the second testing position.

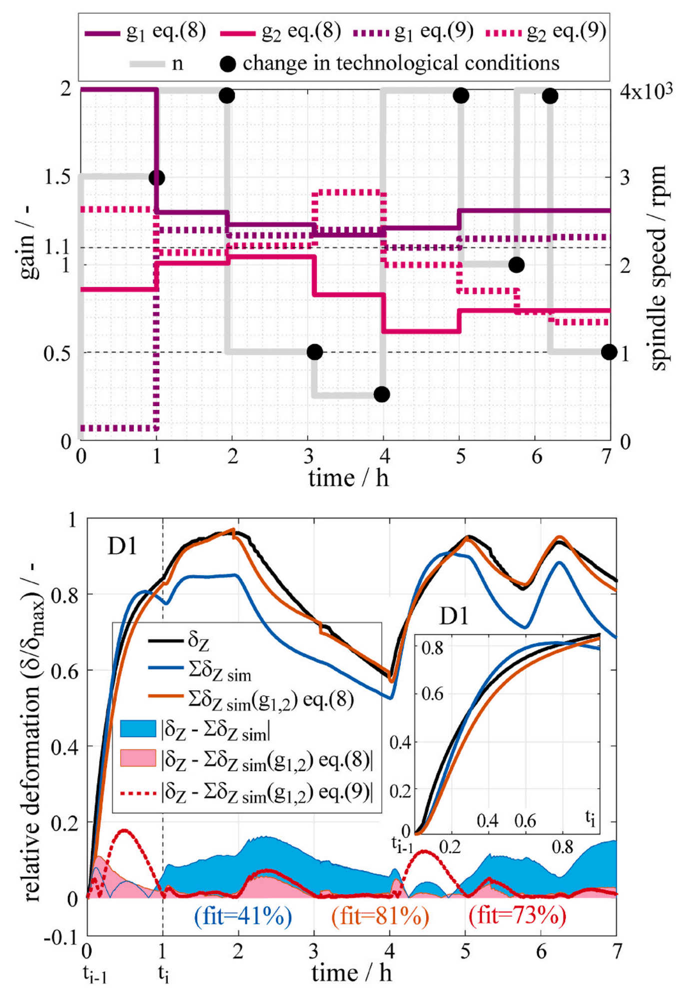

Fig. 8. The course of the optimised gain coefficients (left) and measured uncompensated deformations, approximations and residuals after the indirect and the post-process updated model applications (right) during the verification test of the machine with an exchangeable head in the second testing position.

as a result of the post-process update with characteristic boundaries of gain coefficients to the specified machine configuration and set-up. The benefit of parameter optimisation with characteristic boundaries from equation (8) can be seen from the detail between the beginning and the first hour of the test in the right part of Fig. 8. The characteristic boundaries of the optimised gain coefficients reduce the number of the local extrema of equation (6) solutions and the result tends more towards the optimal solution of the fitness function from equation (7). A similar benefit should be seen between the fourth and fifth hours of the test. In this interval, however, the optimisation worsens the situation after compensation by the initial model. Considering the initial boundaries of the gain coefficients in equation (9) decreases the model efficiency by 4% compared to the characteristic boundaries in equation (8). The deterioration of efficiency is particularly noticeable in the two critical intervals of the test. Calibration of new sub-models describing the spindle speed activity in different machine axis configurations and modularity would be necessary to further increase the compensation model efficiency.

5. Application of the post-process update approach in repetitive production

Post-process adaptation is useful in repetitive production. The second case study on a 5-axis milling centre equipped with an efficiently

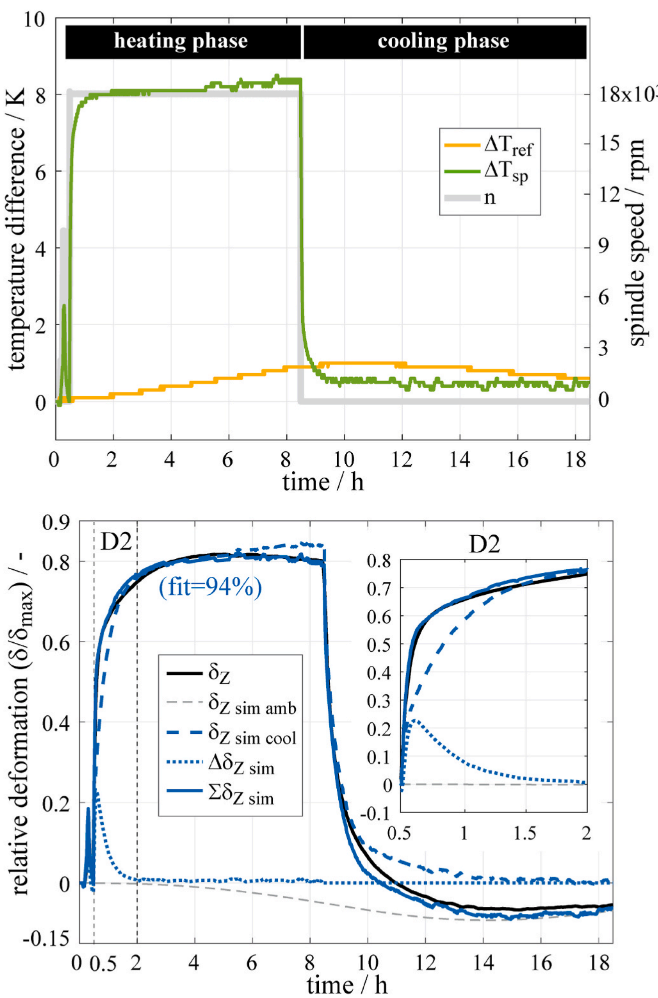

Fig. 9. Development of an indirect compensation model of the 5-axis milling centre's thermo-mechanical behaviour in the Z-axis caused by spindle rotation: input quantities during the calibration measurement (left) and resulting description (right).

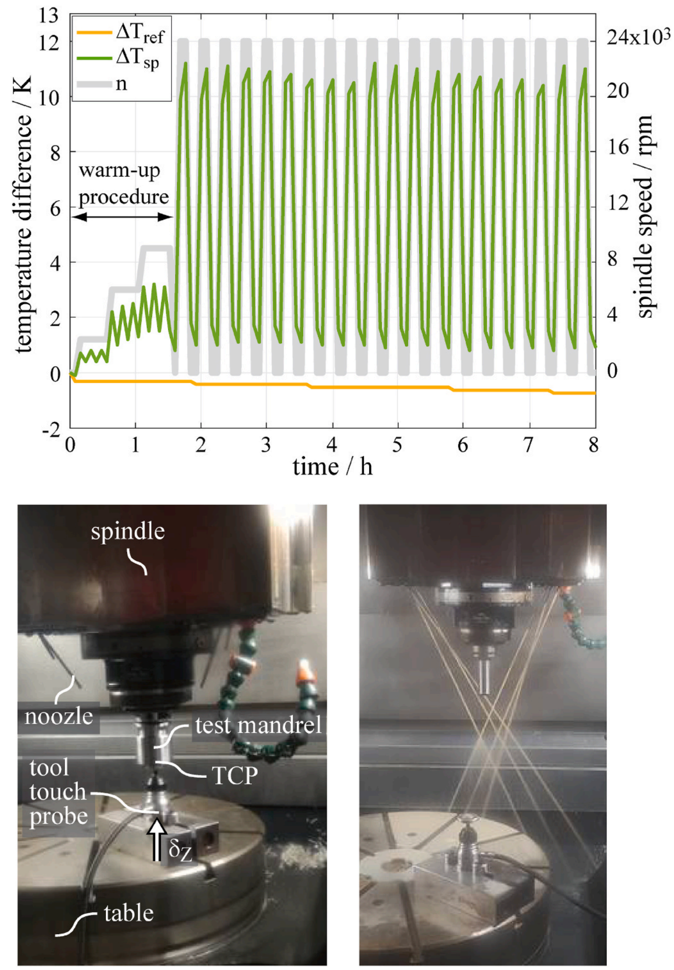

Fig. 10. Input quantities of the compensation model during first repetition of drill-like verification test performed on a 5-axis milling centre (left) and measurement set-up using a tool touch probe and machine under the impact of the process liquid (right).

cooled high-speed spindle (Step-Tec HP 190) presents the entire process from the calibration of the indirect compensation model of thermal errors in the dominant machine direction *Z*, through the model post-process adaptation to the repeated 8-h long NC code. The initial indirect compensation model of the second target machine has the structure from equation (5). Calibration of the model follows the procedure given in Section 3.2 and the results are shown in Fig. 9.

The repetitive code for model verification consists of a spindle warm-up procedure, start-stop drill-like changes in spindle speed, and the presence of process liquid at half the six repetitions that is not part of the calibration setting. A balanced mandrel clamped in the spindle was sensed at a frequency of 5 min^{-1} by a tool touch probe (Heidenhain TT 140) clamped on the table top. The sensing procedure by the tool touch probe took less than 1 min. The principle of TCP measurement, the test set-up and the course of the first drill-like verification test is shown in Fig. 10. The settings follow the MT manufacturer's requirements for a real production case.

The initial indirect compensation model was applied to the first repetition of the drill-like verification test and subjected to the post-process adaptation mechanism described in Fig. 4 with fitness function from equation (9). Both the initial indirect compensation model and the post-process updated model were further applied to two repetitions of the same NC code used for adaptation and three repetitions of the same NC code in addition with the presence of process liquid. The results

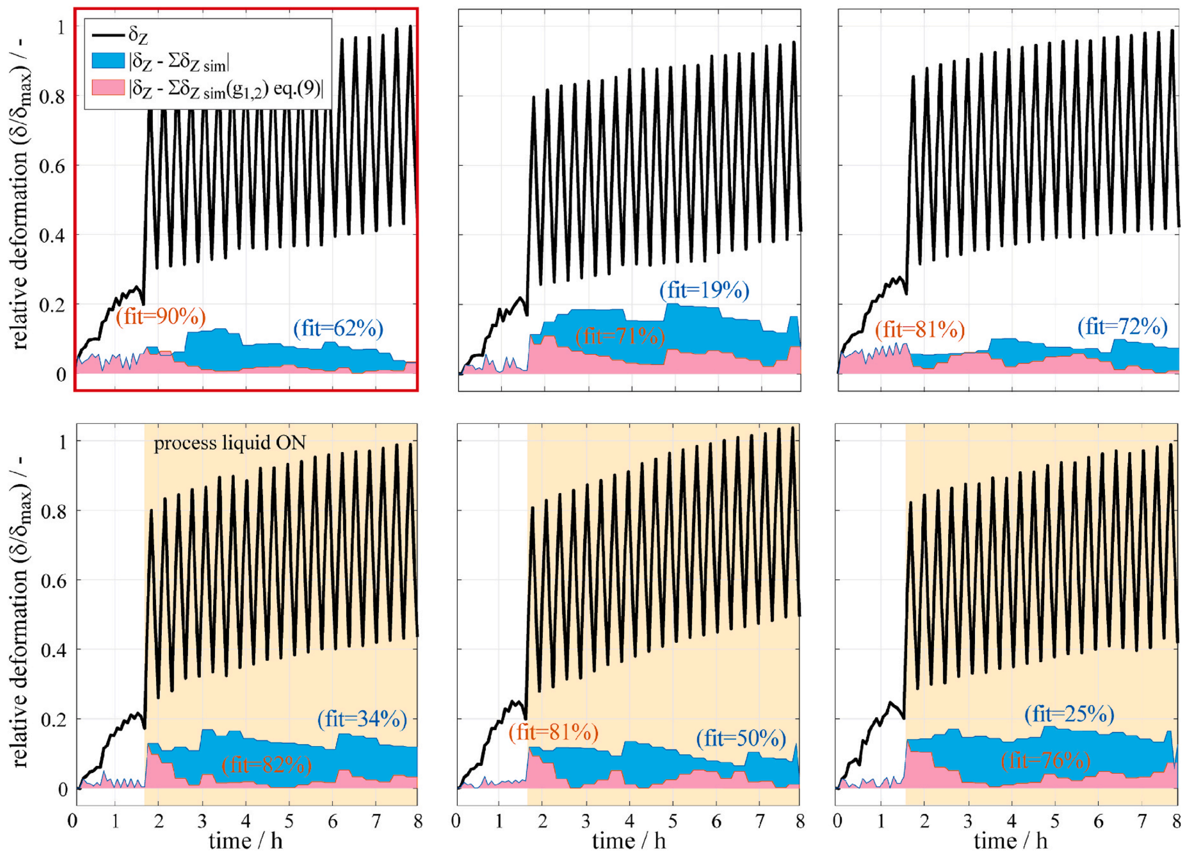

Fig. 11. Measured deformations and residuals after indirect and post-process updated model applications during five separate repetitions of a drill-like verification test on a 5-axis milling centre. The test used to post-process model parameter adaptation is boxed in red. (For interpretation of the references to colour in this figure legend, the reader is referred to the Web version of this article.)

are depicted in Fig. 11 with the first test used for post-process adaptation highlighted.

Average efficiency of initial indirect compensation model reached $\overline{fit} = 40\%$ over six repetition of drill-like verification test. Post-process updated model using fitness function form equation (9) increase the theoretical efficiency during the adaptive procedure, where gain coefficients g_1 and g_2 were optimised, by 28% to a value of $fit = 90\%$. The decrease in the average efficiency of the post-process updated model application for the rest five repetitions of the drill-like test is on average 12% to $\overline{fit} = 78\%$. The average efficiency achieved by the post-process updated model is therefore 38% higher compared to the initial indirect compensation model. From the results of the experimental setup, it can be observed the presence of the process liquid has a negligible impact on the thermal error of the spindle itself. Its importance will be more significant during the removal of cut-off material, cooling of the cutting process and the workpiece.

Data for post-process adaptation can be obtained during machining of the first workpiece with active indirect compensation in the MT control system, i.e. the first workpiece is machined with lower, but still increased, accuracy. The application of the adapted model is carried out on similar workpieces in repeated production.

A different way to obtain the necessary data for updating the model parameters is to machine the workpiece with additional material, measure the functional surfaces, identify and optimise the gain coefficients, enter the coefficients into the model and finish the workpiece. In practice, the cylindricity of the turned/ground workpiece is solved in a similar way.

6. Conclusions

The presented research provides an approach to post-process updating of an indirect compensation model of MT thermal errors. Post-process updating lies on the boundary between indirect compensation method and adaptive compensation combining an indirect model with real time in-process measurements. The approach uses a granular structure of TF-based models and a gain scheduling strategy to update model parameters to areas outside of the calibration range characterised by a nonlinearity and inhomogeneity of the MT thermo-mechanical system. A heuristic method of GA is used to automatically optimise the gain coefficients added to the compensation model. Direct measurements of residual thermal errors at moments of change in technological conditions are the only feedback of the system, minimising disruption to the production process and preserving the integrity of the workpiece surface. This approach is particularly useful in repetitive production, as it significantly increases the efficiency of compensations.

The capabilities of post-process adaptation of thermal error compensation models were demonstrated on two case studies. First, the identification process of an initial indirect compensation model was realised on a heavy-duty milling machine with a horizontal headstock. The initial model approximates the influences of ambient temperature changes and spindle rotation with respect to the differences between heating and cooling phases. The model was calibrated within idle load conditions for the MT in the basic configuration and in one position of the machine axes. The parameters of the initial model were subsequently updated post-process to effectively approximate thermal errors induced by the machine operating in a configuration with an exchangeable spindle head, variable spindle speeds and in different positions of the workspace. The approach's high potential is indicated by an 40%

increase in the average efficiency of the updated model compared to the initial model. The importance of quality input values from system feedback was emphasized. Second, the advantages of the post-process updated model were presented on a repeatedly executed NC program specified by the manufacturer of a 5-axis milling centre equipped with a high-speed spindle and initial indirect compensation model patterned after the previous target machine. The post-process adapted model showed high efficiency of compensation values during application to six repetitions of drill-like experiment with start-stop variation of spindle speed and presence of process liquid. The average efficiency increase of the updated model was 38% compared to the initial model.

The values of the gain coefficients are unique for each setting of the technological parameters. The development of the gain coefficients cannot be generalised, partially because of the different conditions of the processes to which they are optimised. However, in follow-up research, linking the updating gain coefficients with the conditions of a known production process to which they are optimised could enable future application to similar production settings. Within the context of soundly anchored Industry 4.0 principles, the development of smart production systems and horizontal machine monitoring, these visions are real.

Conflicts of interest

The authors declare that they have no known competing financial interests or personal relationships that could have appeared to influence the work reported in this paper.

Acknowledgement

The results were achieved from funds to support the development of Science & Research at the Faculty of Mechanical Engineering of the Czech Technical University in Prague.

Appendix A. Supplementary data

Supplementary data to this article can be found online at https://doi.org/10.1016/j.precisioneng.2024.02.011.

References

[1] Ramesh R, Mannan MA, Poo AN. Error compensation in machine tools - a review: Part I: geometric, cutting-force induced and fixture-dependent errors. Int.J.Mach. Tools Manuf. 2000;40(9):1235–56.
[2] Bryan J. International Status of thermal error research. CIRP Ann.Manuf.Technol. 1990;39(2):645–56. 1990.
[3] Weck M, McKeown P, Bonse R, Herbst U. Reduction and compensation of thermal errors in machine tools. Annals of the CIRP 1995;44(2):589–98.
[4] Deng X-L, Lin H, Wang J-C, Xie C-X, Fu J-Z. Review on thermal design of machine tool spindles. Optics and Precision Engineering; 2018. p. 1415–29.
[5] Jedrzejewski J, Winiarski Z, Kwasny W. Research on forced cooling of machine tools and its operational effects. Journal of Machine Engineering 2020;20(2): 18–38.
[6] Kumar TS, Glänzel J, Tehel R. Experimental validation of characteristic diagram - parameterization for environment-induced thermal interactions on machine tools in a climate chamber. Procedia CIRP 2021;99:63–8.
[7] Ramesh R, Mannan MA, Poo AN. Error compensation in machine tools - a review: Part II: thermal errors. Int.J.Mach.Tools Manuf. 2000;40(9):1257–84.
[8] Brecher C, Wissmann A, Klein W. Compensation of thermo-dependent machine tool deformations due to spindle load based on reduced experimental procedure and modeling effort – Synthesis between direct and indirect compensation. In: 8th international Conference on high speed machining. France: Metz; 2010.
[9] Gao W, Haitjema H, Fang F, Leach R, Cheung C, Savio E, Linares J. On-machine and in-process surface metrology for precision manufacturing. CIRP Annals 2019;68(2): 843–66.
[10] Mayr J, Jedrzejewski J, Uhlmann E, Alkan Donmez M, Knapp W, Härtig F, Wendt K, Moriwaki T, Shore P, Schmitt R, Brecher C, Würz T, Wegener K. Thermal issues in machine tools. CIRP Ann.Manuf.Technol. 2012;61(2):771–91.
[11] Li Y, Yu M, Bai Y, Hou Z. A review of thermal error modeling methods for machine tools. Applied Sciences; 2021. p. 16.
[12] Li Y, Zhao W, Lan S, Ni J, Wu W, Lu B. A review on spindle thermal error compensation in machine tools. Int J Mach Tool Manufact 2015;95:20–38.
[13] Zapłata J, Pajor M. Piecewise compensation of thermal errors of a ball screw driven CNC axis. Precis Eng 2019;60:160–6.
[14] Mayr J, Ess M, Weikert S, Wegener K. Compensation of thermal effects on machine tools using a FDEM simulation approach. Proceedings of Lamdamap 2009;9.
[15] Hernández-Becerro P, Spescha D, Wegener K. Model order reduction of thermo-mechanical models with parametric convective boundary conditions: focus on machine tools. Comput Mech 2021;67:167–84.
[16] Xiao J, Fan K. Research on the digital twin for thermal characteristics of motorized spindle. Int J Adv Des Manuf Technol 2022;119(7).
[17] J. W. Li, W. J. Zhang, G. S. Yang, S. D. Tu and X. B. Chen, "Thermal-error modeling for complex physical systems: the-state-of-arts review," Int J Adv Des Manuf Technol, vol. 42, no. 1, p. 168-179, 17 6 2008..
[18] Naumann C, Glänzel J, Putz M. Comparison of basis functions for thermal error compensation based on regression analysis – a simulation based case study. Journal of Machine Engineering 2020;20(4):28–40.
[19] Brecher C, Hirsch P, Weck M. Compensation of thermo-elastic machine tool deformation based on control internal data. CIRP Ann.Manuf.Technol. 2004;53(1): 299–304.
[20] Mize C, Ziegert J. Neural network thermal error compensation of a machining center. Precis Eng 2000;24:338–46.
[21] Zimmermann N, Mayr J, Wegener K. Extended discrete R-Test as on-machine measurement cycle to separate the thermal errors in Z-direction. In: Proceedings of special interest group meeting: thermal issues, Aachen; 2020.
[22] Mayr J, Blaser P, Ryser A, Hernandez-Becerro P. An adaptive self-learning compensation approach for thermal errors on 5-axis machine tools handling an arbitrary set of sample rates. CIRP Annals - Manufacturing Technology; 2018. p. 551–4.
[23] Zimmermann N, Breu M, Mayr J, Wegener K. Autonomously triggered model updates for self-learning thermal error compensation. CIRP Annals 2021;70(1): 431–4.
[24] Naumann C, Glänzel J, Dix M, Ihlenfeldt S, Klimant P. Optimization of characteristic diagram based thermal error compensation via load case dependent model updates. Journal of Machine Engineering 2022;22(2):43–56.
[25] Mareš M, Horejš O, Hornych J, Smolík J. Robustness and Portability of machine tool thermal error compensation model based on control of Participating thermal sources. Journal of Machine Engineering 2013;13(1):24–36.
[26] Rugh WJ, Shamma JS. Research on gain scheduling. Automatica 2000;36(10): 1401–25.
[27] ISO 230-3. 2020 Test code for machine tools — Part 3: Determination of thermal effects. 3 ed. Genf, Switzerland: International Organisation for Standardization; 2020. p. 50.
[28] Mareš M, Horejš O, Havlík L. Thermal error compensation of a 5-axis machine tool using indigenous temperature sensors and CNC integrated Python code validated with a machined test piece. Precision Engineering; 2020. p. 21–30.
[29] Stoop F, Mayr J, Sulz C, Kaftan P, Bleicher F, Yamazaki K, Wegener K. Cloud-based thermal error compensation with a federated learning approach. Precis Eng 2023; 79:135–45.
[30] Bart H. Transfer functions and operator theory. Lin Algebra Appl 1986;84:33–61.
[31] Fraser S, Attia MH, Osman MOM. Modelling, identification and control of thermal deformation of machine tool structures, Part 1: concept of generalized modelling. J.Manuf.Sci.Eng.Trans.ASME 1998;120(3):623–31.
[32] Ljung L. System identification Toolbox™ User's Guide. The MathWorks; 2015.
[33] Houck CR, Joines JA, Kay MG. A genetic algorithm for function optimalization: a Matlab implementation. North Carolina State University; 1999. p. 14.